Carbon 1969, Vol. 7, pp. 1–8. Pergamon Press. Printed in Great Britain

GROWTH OF SINGLE-CRYSTAL GRAPHITE BY PYROLYSIS OF ACETYLENE OVER METALS

A. E. B. PRESLAND

Department of Chemical Engineering and Chemical Technology, Imperial College, London S.W.7, England

and

P. L. WALKER, JR.

Department of Materials Science, The Pennsylvania State University, University Park, Penn. 16802, U.S.A.

(*Received* 4 *October* 1968)

Abstract—Carbon has been prepared by pyrolysis of acetylene over foils of platinum and nickel heated to 1000°C. The deposits are shown to consist of three-dimensionally ordered graphite, with crystal dimensions in the *a*-direction (parallel to the substrate surface) as large as 5 μ. Optical and electron microscopy has been used to show that the graphite nucleates preferentially at substrate grain boundaries and kink sites. In the case of nickel, surface steps also influence growth, and the graphite film produced by complete coverage of the substrate is under compressive stress. Mechanisms for the formation of graphite by this means are discussed, and evidence is provided which indicates that precipitation from solution in the substrate cannot be involved.

1. INTRODUCTION

The formation of crystalline graphite is a process of considerable interest. The largest single crystals are found in geological deposits (e.g. Ticonderoga, Madagascar) where they may have crystallized from solution in the mineral matrix. Many transition metals, too, dissolve significant quantities of carbon at high temperatures, which precipitates as graphite on cooling. The best-known example of this is the 'kish' which forms during steel-making. Austerman *et al.*[1] have used melts of iron and nickel to produce large, relatively perfect graphite crystals in this way.

Transition metals have also been used to lower the temperature of graphitization of commercial carbons[2]. It has been suggested that carbon either dissolves in, or forms a carbide with, these so-called graphitization catalysts; and that subsequently, either by precipitation from solution, or by dissociation of the carbide, this carbon reappears as graphite.

By anology with the growth of thin single crystal metal films, it might be supposed that an alternative approach to the production of crystalline graphite would be to deposit carbon from the vapor phase on to a suitable substrate, at a temperature high enough to give adequate mobility. A pyrolytic carbon with almost theoretical density, three-dimensional ordering and a *c*-spacing of 3·354 A has in fact been reported[3]. Such carbons usually have a turbostratic structure, however, raising the substrate temperature does not significantly improve this. Most pyrolytic carbons are deposited on an existing graphite surface, whereas there is some evidence to suggest that a metal surface may be more effective in providing the required mobility.

Thus, studies of the oxidation of single crystal graphite using metal catalysts[4, 5]

have shown that some of these metals (e.g. Pt, Ag) are extremely mobile on the graphite basal plane, indicating a very low interfacial energy.

Furthermore, Banerjee *et al.*[6] found that carbon films deposited on nickel by the pyrolysis of C_3O_2 were more graphitic than would have been expected at the temperature used. Irving and Walker[7] evaporated carbon in vacuo on to foils of Mo, W, Pt and Ta heated to 1000°C and obtained enhanced graphitization in all cases, as compared with carbon evaporated on to metallic substrates at room temperature. Pt and Ta, in particular, gave spot patterns in selected area electron diffraction, indicating graphite crystal diameters (in the *a*-direction) in excess of 1000 A.

Karu and Beer pyrolyzed methane over foils of nickel heated to temperatures in the range 900–1100°C and obtained thin film deposits, which they stripped and examined by transmission electron diffraction[8]. These films gave selected area diffraction patterns corresponding to graphite single crystals.

In view of this evidence, it was decided to attempt the production of thin films of crystalline graphite by the pyrolysis of acetylene over metal foils. Acetylene was used for this purpose since it is thought to play a key role as an intermediate in the formation of carbon from all gaseous organic compounds[9]. Nickel and platinum foils were used as substrates as they are good dehydrogenating agents. Optical and electron microscopy were employed to characterize the deposits and to obtain information about their nucleation and growth.

2. EXPERIMENTAL

The Ni foils used were 0·0025 in. thick, polycrystalline, with a surface finish sufficiently rough to give non-specular reflection. The Pt foil was 0·010 in. thick, polycrystalline, with an extremely high polish. Both foils were reagent grade; they were degreased in acetone, and cleaned by dipping in conc. HCl, followed by lengthy washing in distilled water.

Strips of foil about 5×1 cm were clamped between the electrodes of an Elion vacuum unit, which was then pumped to a pressure of between 5×10^{-5} and 5×10^{-6} Torr. Current was passed through the foil until the temperature at the center was approximately 1000°C, as measured with a Leeds and Northrup disappearing filament pyrometer. For each run, the foil was held in vacuo at this temperature for not less than 15 min, since Karu and Beer reported[8] that vacuum annealing was a necessary prerequisite for the production of graphite films. The foil was then allowed to cool to room temperature in vacuo, and cylinder acetylene admitted to the work chamber via an air admittance valve.

Karu and Beer claimed that all their pyrolyses were carried out using methane at a pressure of between 1–10 μ, as measured on a cold cathode ionization gauge. Initial experiments by the present authors, using both methane and acetylene at pressures of 1–50 μ gave completely negative results, in that no visible deposit could be obtained even after 1 hr pyrolysis at 1000°C. Clearly higher pressures were required, but the vacuum apparatus could not be maintained at a constant pressure in excess of 50 μ. Eventually the following technique was used, and proved successful, although interpretation of the results was rendered more complex. With the work chamber being pumped by the diffusion pump and the metal foil at room temperature, acetylene was admitted until the pressure rose to about 20 μ. The foil was then heated to 1000 ± 25°C and the flap valve above the diffusion pump closed. With the pump cut off and acetylene continuing to flow in, the pressure in the work chamber rose rapidly; at no time, however, did it exceed about 1 Torr. The foil temperature was continuously adjusted manually, to take account of the increasing gaseous thermal

conduction. At the end of the desired pyrolysis time, the foil was rapidly cooled to room temperature by cutting off the current and the work chamber pumped out again.

The surface of each foil was first examined with a metallurgical microscope. The central region of the foil was then cut out and the pyrolytic deposit stripped by dissolution in an appropriate solvent. For Ni this was conc. HCl, while Pt was left overnight in a Petri dish of conc. HCl containing one drop of conc. HNO_3. After thorough washing in distilled water, small pieces of the deposit were mounted on grids and examined by transmission electron microscopy and diffraction.

3. RESULTS

3.1 *Platinum*

3.1.1 *Optical microscopy.* Figure 1 is a low-magnification optical micrograph of a platinum foil after 20 min pyrolysis. Every grain boundary was decorated with carbon, and considerable deposition had also taken place at points within the grains, giving rise to an overall nucleation density which varied from grain to grain. These nucleation points were usually randomly distributed but were sometimes arranged in sets of parallel straight lines (Fig. 2). In one or two instances, low-angle boundaries also appeared to be decorated (Fig. 3). Some of the random deposits were large enough to be described as patches (Fig. 3); when these were situated in a region of high nucleation density, they were surrounded by a partially or completely denuded zone (Fig. 4). Groups of short, straight lines were also observed, parallel within a single grain (Fig. 5). In some cases, considerable grain boundary migration had clearly taken place (Fig. 6), one position of the boundary being heavily decorated with carbon while the other was visible by surface grooving (or, in some cases, by a light carbon deposit).

3.1.2 *Electron microscopy.* The deposit stripped from the Pt surface was found to be a continuous, electron-transparent film, supporting all the denser features which had been evident in the optical microscope. Selected area diffraction from the continuous film gave a pattern consisting of two weak diffuse rings at 2·13 and 1·23 A, corresponding to a pyrolytic carbon with its c-axis predominantly perpendicular to the film plane and an L_a value of about 50 A. The grain boundary deposit (Fig. 7), however, gave in addition to the amorphous carbon pattern a single hexagonal spot pattern completely consistent with single crystal graphite (from a selected area $\sim 25\ \mu^2$). The crystallographic nature of the deposit boundaries and the occasional moiré patterns observed provided further evidence for this. Selected area diffraction, the tendency towards regular morphology, and the occasional presence of extinction contours suggested that the patch deposits (Fig. 8) were also of single crystal graphite. This was confirmed by dark field microscopy.

3.2 *Nickel*

3.2.1 *Optical microscopy.* The nickel foil surface appeared, under the optical microscope, to be very different from that of platinum, after both had received the preliminary heat treatment. Whereas the effect of the latter on platinum was merely to produce grain boundary grooving, the annealed Ni surface showed, in addition, extensive step and terrace formation. This surface structure had a marked effect on the deposit morphology. Thus, nucleation occurred along single steps and at grain boundaries (Fig. 9). At a later stage considerable lateral intergrowth had occurred, and the tentacular appearance of the deposit boundary indicated that growth along steps was favored (Fig. 10).

As the deposit thickness increased, the underlying step structure of the substrate could no longer be seen; the upper surface of the deposit took on the 'polygonal net-

work' appearance shown at *C* in Fig. 10. This polygonal network is clearly in evidence in Fig. 11, which shows the appearance of the foil when completely covered with deposit. The features at *D* are 'blisters', i.e. raised areas of deposit film which have parted company with the underlying substrate.

3.2.2 *Electron microscopy.* After $3\frac{1}{2}$ min pyrolysis, the stripped deposit had the appearance of a lacework of individual crystals (Fig. 12). The original grain boundaries of the substrate can be seen, decorated by enhanced deposition. The inset electron diffraction pattern was obtained from an area of the deposit corresponding to one such substrate grain. The graphite is clearly microcrystalline, albeit with a tendency to preferred *a*-axis orientation. Figure 13 shows a higher magnification micrograph of one of the larger graphite crystals, in which can be seen a number of low-angle boundaries. The equivalent diffraction pattern (inset) confirms this.

After 10 min pyrolysis, the diffraction pattern had become more spotty, indicating an increase in crystal size (Fig. 14). The graphite crystals were now becoming increasingly acicular in shape, with the long axes lying parallel to one another (Fig. 15).

The continuous film formed after 33 min pyrolysis proved to be rather thick for examination in transmission; in view of the large extinction distance for graphite, the film thickness was probably of the order of 2000–5000 A. Figure 16 shows that the film contained an extensive tilt-boundary network. Some of these tilt boundaries may correspond to the polygonal structure observed in the optical microscope. Moiré patterns were also observed (e.g. at *M*, Fig. 17), indicating the presence of twist boundaries between overlapping crystals. The selected area diffraction pattern (Fig. 18) corresponded to single crystal graphite, with additional weak continuous rings through the $10\bar{1}0$ and $11\bar{2}0$ reflections, caused by the presence of some amorphous carbon.

4. DISCUSSION

4.1 *Effect of hydrocarbon pressure*

Whatever the detailed mechanisms involved in the dehydrogenation of acetylene to carbon, it is clear that the rate of carbon production must increase with pressure and must, therefore, in the experiments described increase with pyrolysis time.

The requirements for single crystal formation are (i) low rate of nucleation, (ii) low rate of growth, (iii) high mobility. In these experiments the surface temperature, and hence the mobility, were kept constant. The carbon deposition rate was steadily increasing, however; and it must be assumed that for some time after the start of pyrolysis the combination of deposition rate and mobility was such as to permit the formation of crystalline graphite. This graphite was nucleated heterogeneously at favored sites on the substrate surface. Eventually, carbon must have been produced so rapidly that an amorphous deposit was formed homogeneously over the surface. On stripping, this acted as an extraction replica, bearing the localized graphitic deposits formed earlier in the pyrolysis.

4.2 *Nucleation*

4.2.1 *Grain boundary nucleation.* The fact that both platinum and nickel grain boundaries act as favorable sites for the nucleation of graphite could be due to (a) the local change in topography at the intersection of the grain boundary with the surface, (b) the action of the grain boundary itself as a preferred route for the diffusion of carbon, or of point defects, or (c) the effect of localized impurity concentrations as a result of segregation to the boundary. Some light is thrown on this by consideration of the effects shown in Fig. 6 where the grain boundary has clearly migrated during pyrolysis.

This configuration could arise in two ways; either site *A* or site *B* (Fig. 6) could represent the final position of the grain boundary. On the whole, migration from A to B seems

Fig. 1. Optical micrograph of surface of Pt foil after 20 min pyrolysis, showing decorated grain boundaries and variable nucleation density (154×).

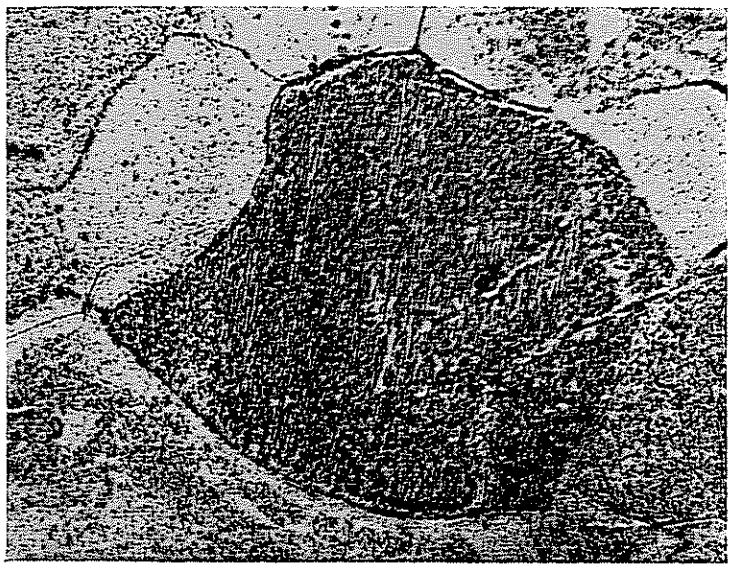

Fig. 2. Striated nucleation on Pt (630×).

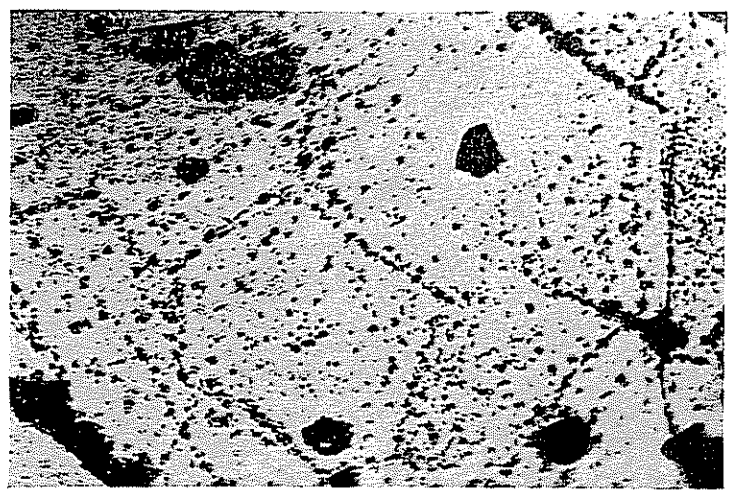

Fig. 3. Sub-grain boundary decoration of Pt (630×).

[*Facing page* 4]

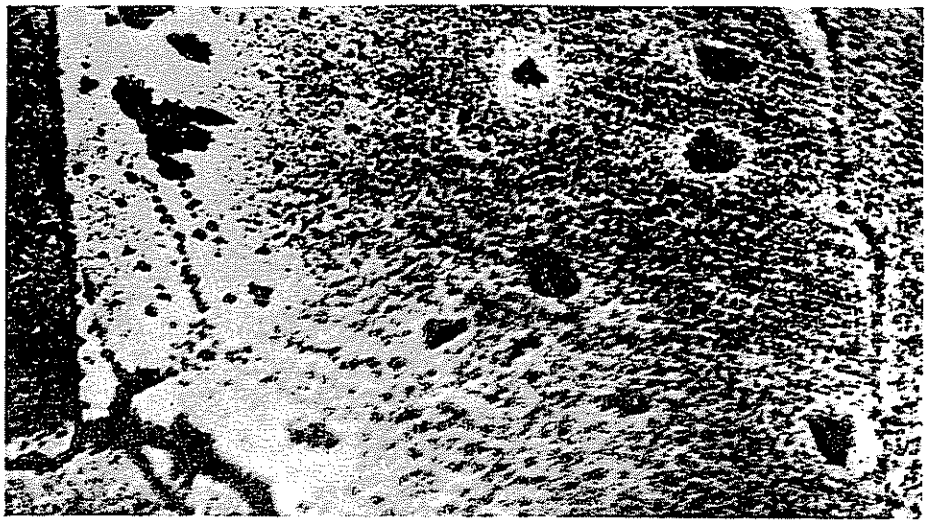

Fig. 4. Denuded zones around grain boundaries and patch deposits on Pt (630×).

Fig. 5. Linear deposits on Pt (630×).

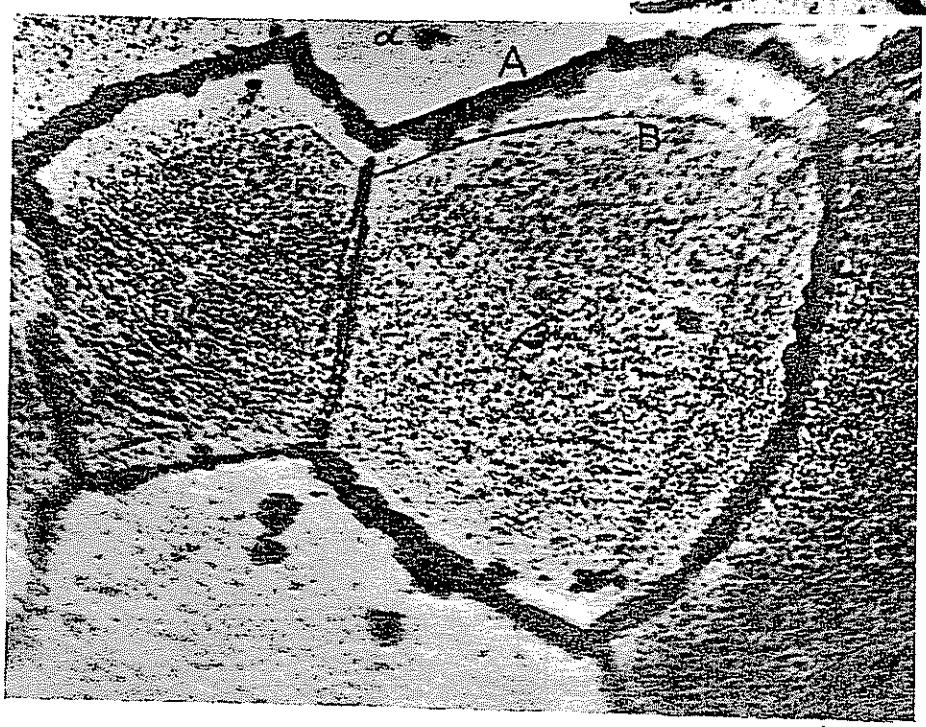

Fig. 6. Effect of grain boundary migration of Pt (630×).

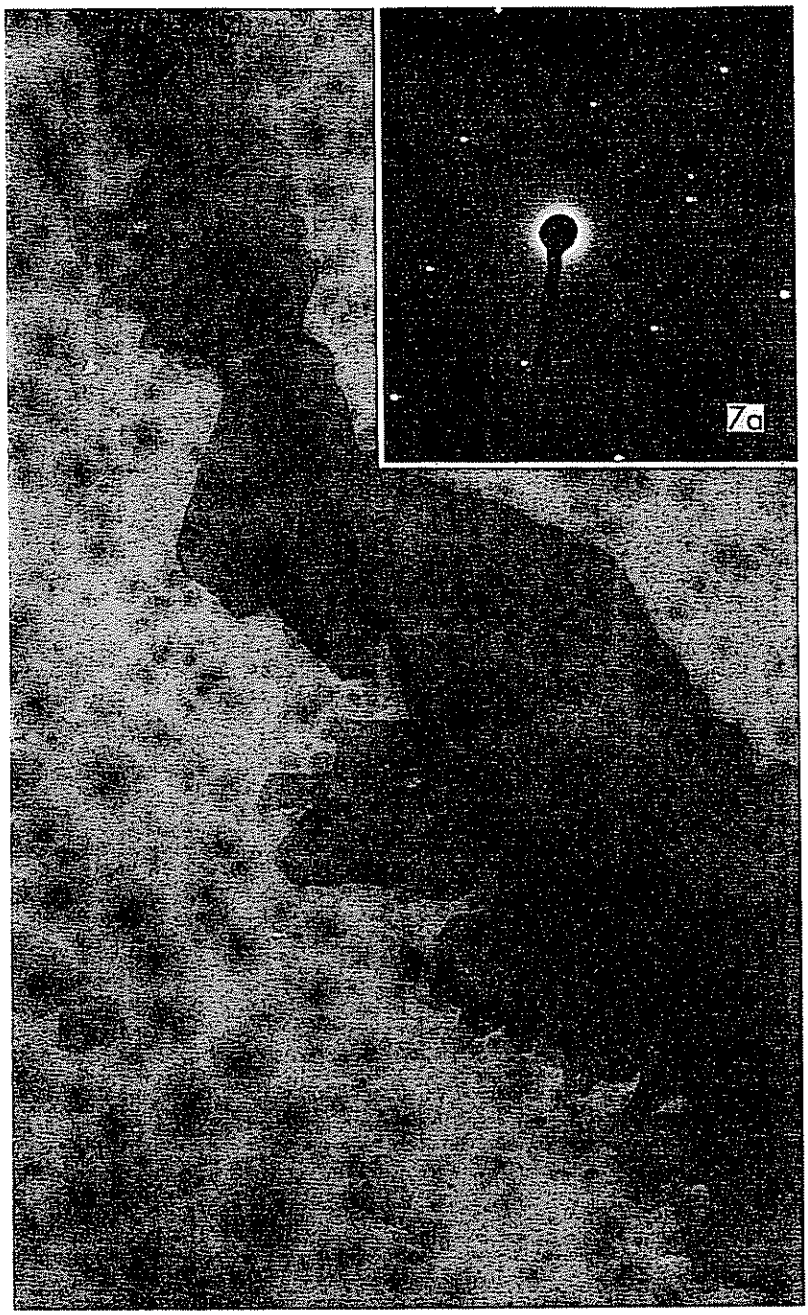

Fig. 7. Electron micrograph of grain boundary deposit stripped from Pt (8000×). (*Inset:* Equivalent selected area electron diffraction pattern.

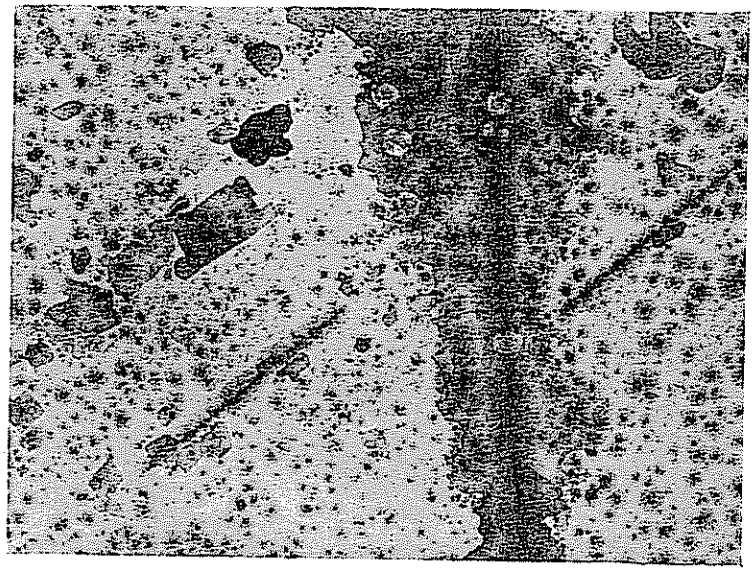

Fig. 8. Grain boundary, patch and linear deposits on Pt (3500×).

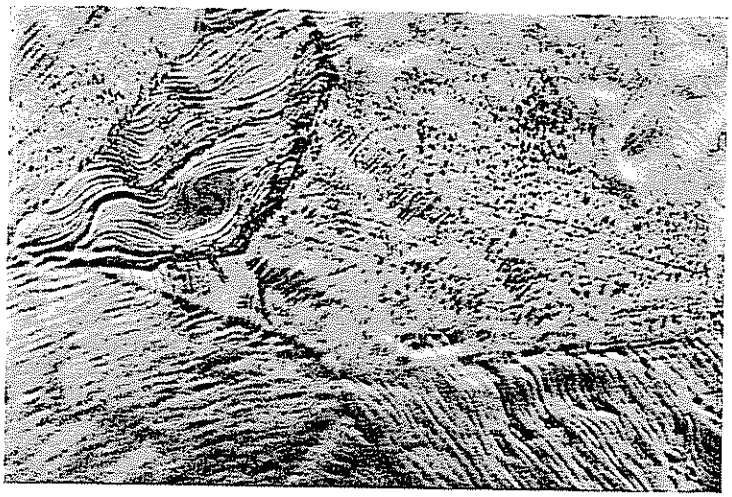

Fig. 9. Optical micrograph showing grain boundary and step nucleation on Ni (630×).

Fig. 10. Step growth on Ni. Note polygonal network formation at *C* (630×).

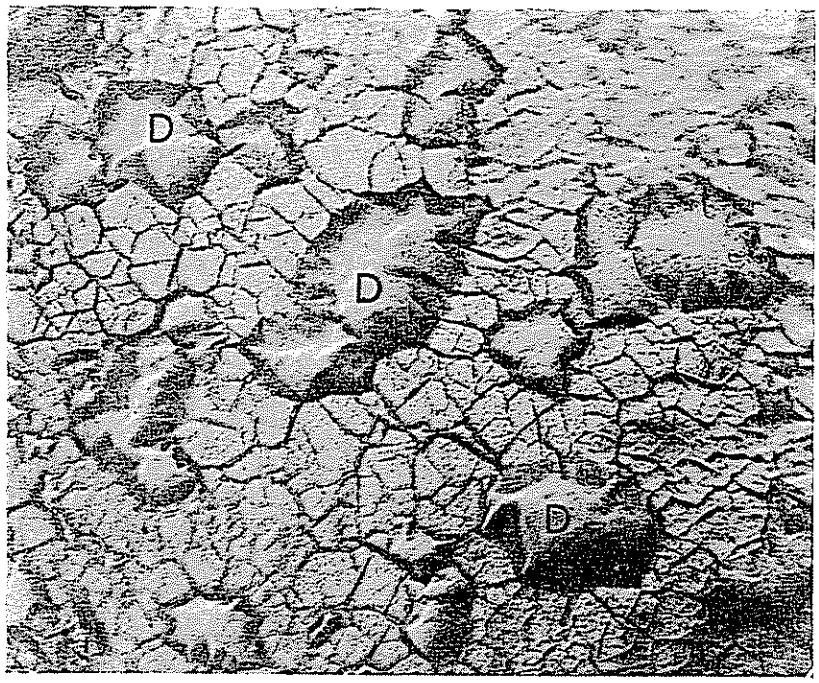

Fig. 11. Continuous graphite film on Ni, showing polygonal network and raised 'blisters' at *D* (630×).

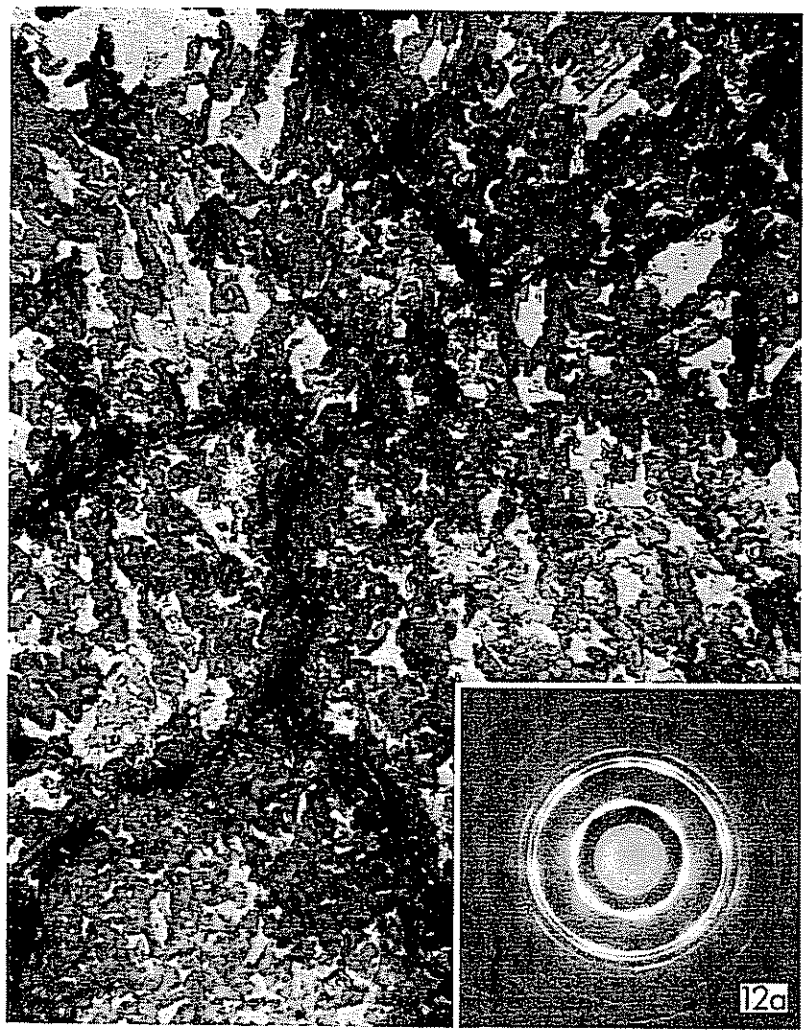

Fig. 12. Electron micrograph of deposit stripped from Ni after 3-1/2 min pyrolysis (2500×). (*Inset:* Electron diffraction pattern from area corresponding to one substrate grain of Ni.)

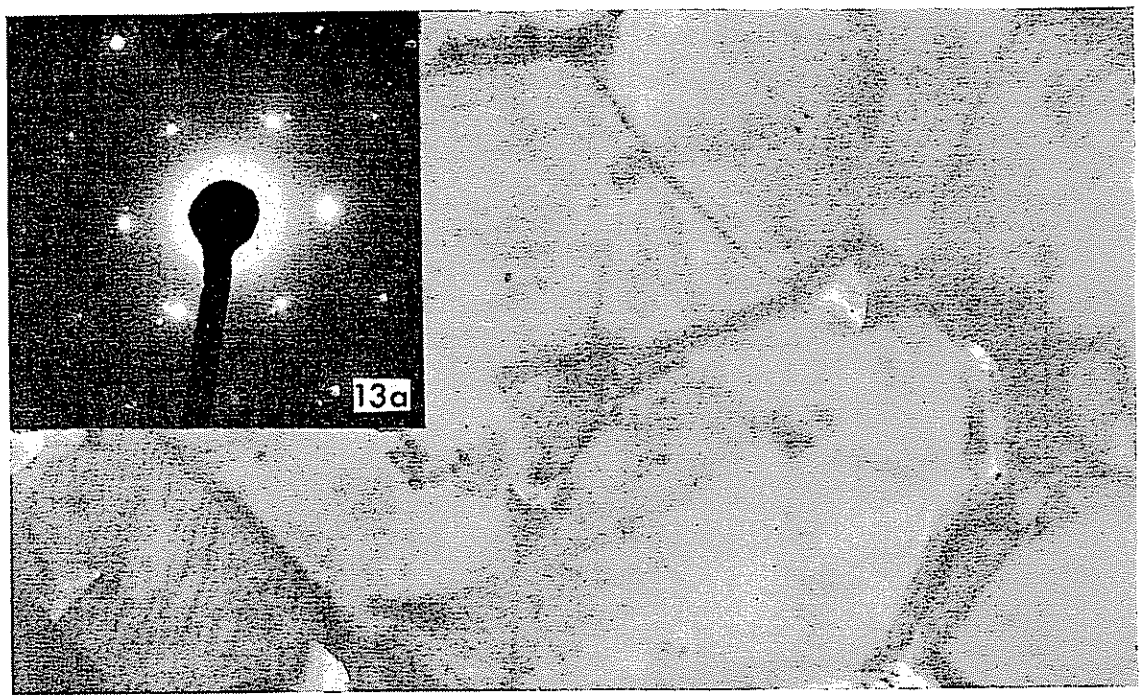

Fig. 13. Low-angle boundaries in a single graphite crystal formed on Ni (21,000×). (*Inset:* Equivalent selected area electron diffraction pattern of graphite crystal formed on Ni.)

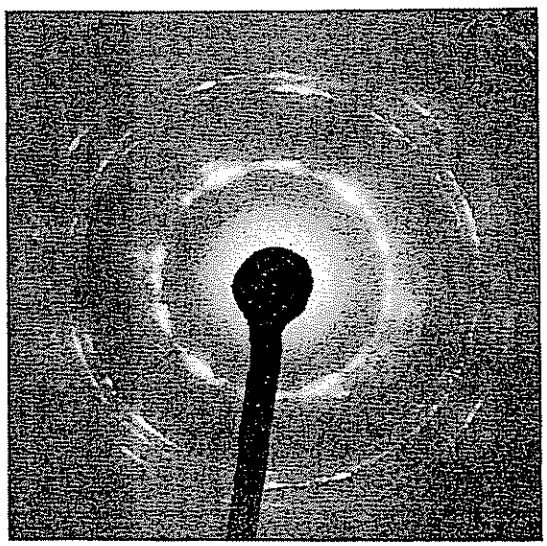

Fig. 14. Electron diffraction pattern of graphite deposit stripped from Ni after 10 min pyrolysis.

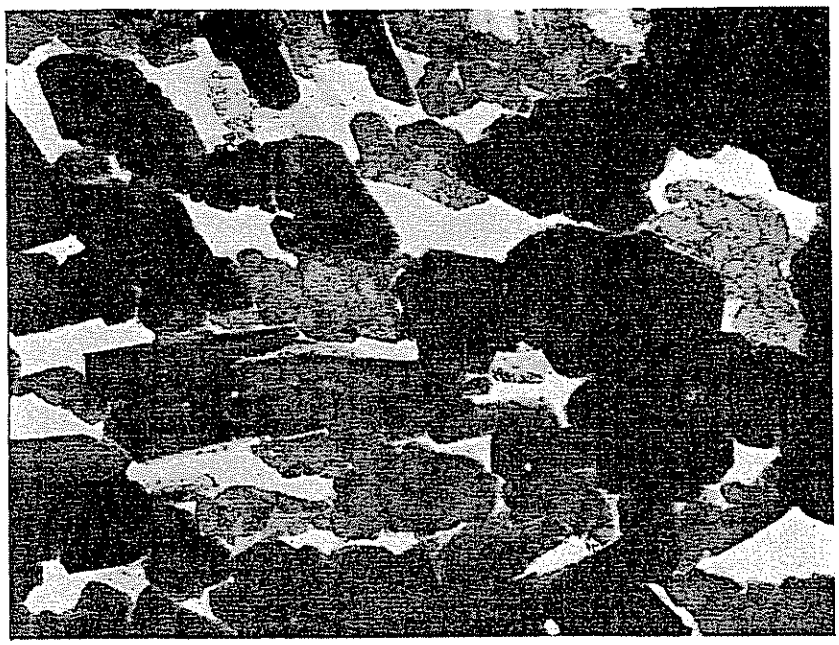

Fig. 15. Acicular crystals of graphite formed on Ni (conditions as for Fig. 14) (3500×).

Fig. 16. Transmission electron micrograph of continuous graphite film stripped from Ni, showing tilt boundary network (4800×).

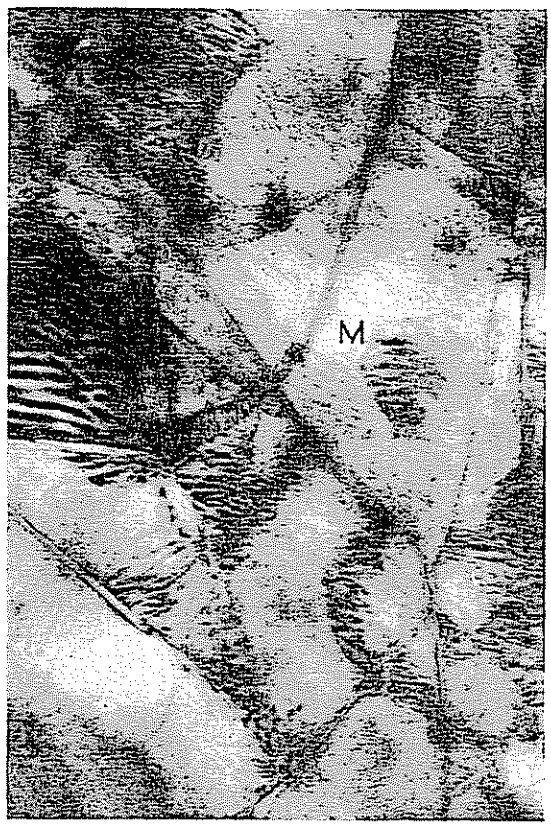

Fig. 17. Moiré patterns (e.g. at M) indicating relative rotation between overlapping graphite crystals formed on Ni (17,600×).

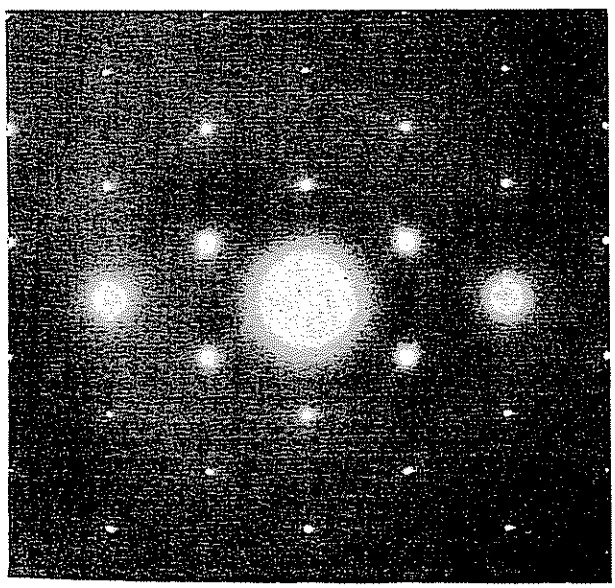

Fig. 18. Selected area electron diffraction pattern of graphite crystals (corresponding to Fig. 17) formed on Ni.

somewhat more likely, for the following reasons:

(i) Grain boundaries migrate towards their center of curvature.

(ii) If the boundary had moved from B to A, it would be necessary to assume that the boundary could move faster than the thermal groove at the surface could be eliminated by smoothing. In view of the fact that surface diffusion coefficients are normally at least as high, if not higher than those for grain boundary diffusion, this appears unlikely.

(iii) The nucleation density in the region between A and B corresponds to that outside A (i.e. on grain α) rather than that inside B (on grain β). Since this density is a function of grain orientation (perhaps through the kink site density, see (4.2.2), the region AB must have changed either from orientation β to orientation α very early in the pyrolysis, before significant amounts of graphite had been deposited on area AB, or from orientation α to β at a much later time, when amorphous carbon was being deposited homogeneously over the entire surface. In the latter case, however, no decoration of the boundary when in the final A position could occur.

The most probable interpretation of areas such as Fig. 6 is, therefore, as follows. In the very early stages of pyrolysis, graphite nucleates along the substrate grain boundary at A before there is any significant deposition on the surface of grain β. The boundary then migrates inward; and while it is moving, further deposition on it is inhibited (possibly because it moves rapidly). Its motion, of course, converts β into α, changing the local kink site density. If the boundary comes to a halt while graphite is still being (heterogeneously) deposited, it will be lightly decorated; if it stops during the amorphous carbon (homogeneous) regime, only a thermal groove will be formed at the intersection with the surface. In either case, this now corresponds to site B. While all this is taking place, extensive further deposition of graphite is occurring at the original nuclei formed at site A, followed eventually by an overall coating of amorphous carbon.

4.2.2 *Surface nucleation.* If the grain boundary/surface intersection is a preferred nucleation site, it might be expected that the point of emergence of a dislocation would be similarly favored. The surface nucleation density over platinum was found to vary between 10^6 and $10^8\,cm^{-2}$, which seems too high to correspond to the dislocation density in a fully-annealed f.c.c. metal. In any case, thermal annealing would have led to polygonization, at least; and although occasional examples interpretable as decoration of low-angle boundaries were found (Fig. 3), the distribution of nuclei was usually either random, or heavily striated, as in Fig. 2. Thus some other site must be operative.

Those substrate grains whose outer surface corresponded to a high-index plane would, on thermal annealing, be resolved into a multiple-faceted surface, which would provide a high density of kink sites suitable for nucleation [10]. Further, these sites would often lie in parallel rows, thus accounting for the observed striations. The density of these kink sites would depend on the orientation of the initial substrate grain and would, therefore, vary widely.

4.3 *Growth morphology*

The growth of graphite on both platinum and nickel takes place by the lateral extension of island nuclei. In the case of nickel, however, this growth is strongly influenced by the surface topography, in particular by the step and terrace structure of the substrate. Thus Fig. 10 shows that growth takes place mainly along the steps, and the lath-shaped graphite crystals in Fig. 15 were presumably formed in this way.

4.4 *Epitaxy*

The formation of a single crystal overgrowth by deposition on to a crystalline substrate is usually the result of an epitaxial relationship between overgrowth and substrate. Thus, it is natural to enquire whether this is the case here. The two metals used for the substrate were both f.c.c. and both in the form of cold-rolled foil so that although polycrystalline they may have had a similar preferred orientation, which would have been (110)/[$\bar{1}$12][11]. Thus, most grains would have had a surface plane close to (110), the symmetry of which is not particularly conducive to epitaxial growth of a hexagonal structure such as graphite. However, thermal etching may have led to the formation of surface steps involving lower energy planes such as (111) which, with their hexagonal symmetry, would have been much more likely to provide a suitable site for epitaxial growth.

In the case of platinum, however, the grain boundaries were the prime source of single crystal graphite, extending on either side of the true boundary. Even if the substrate grain on one side were in the appropriate orientation for epitaxy, it is unlikely that the correct relationship would be maintained on the other side. Since most of the grain boundaries were decorated with crystalline graphite in this way, it appears either that some of the latter grew non-epitaxially or, possibly, that the density of (111) facets was higher in the vicinity of the grain boundaries. The presence of patches of graphite of more or less crystallographic shape (see Fig. 8) may point to an epitaxial effect, although this particular morphology could be due to the step structure of the substrate surface.

The graphite deposits on nickel provide even less evidence for an epitaxial relationship. Comparison of Figs. 12, 14 and 18 shows that while the *c*-axis is normal to the substrate surface from the early stages of pyrolysis, the *a*-axis orientation is almost random at first and steadily improves as surface coverage increases. This, in turn, implies recrystallization of the graphite.

Clearly more experimental evidence is required to determine whether this type of graphite overgrowth is epitaxial or not.

4.5 *Microstructure of the continuous graphite film*

Complete coverage of the substrate surface was achieved only for nickel. The polygonal network and the 'blisters' shown in Fig. 11 can be accounted for in the following way. The graphite overgrowth which forms at 1000°C is firmly keyed into the heavily terraced Ni surface; on cooling to room temperature, stresses are set up in the graphite due to differential contraction. Since the graphite *c*-axis is everywhere normal to the surface, the relevant expansion coefficient is that for the *a*-axis, which is negative up to about 900°C. Extrapolating the results of Nelson and Riley[12], a value of $\Delta l/l$ at 1000°C of about 7×10^{-5} would be obtained. This should be compared with a $\Delta l/l$ for Ni at 1000°C of $1{\cdot}55 \times 10^{-2}$[13]. The thickness of the Ni substrate was ~100x that of the graphite overgrowth; assuming no deformation of the former, a compressive strain of about $1{\cdot}5 \times 10^{-2}$ would be imposed on the latter, which would be more than sufficient to give rise to plastic deformation. The only mode of deformation of graphite single crystals at room temperature is by the motion of basal dislocations, giving rise to twinning and tilt boundary formation[14]. Since the compressive stresses would not be uniaxial but randomly distributed in the plane of the film, the twins and tilt boundaries would form just the sort of polygonal network observed. In regions where the adhesion of the overgrowth to the substrate was poor, the film could accommodate the compressive stresses by buckling away from the substrate, giving rise to the 'blisters' shown in Fig. 11.

4.6 *Graphite formation mechanisms*

Three possible mechanisms may be suggested to account for the growth of crystalline graphite in the experiments which have been described. For convenience these mechanisms will be described as 'chemical', 'thin film', and 'metallurgical' respectively.

4.6.1 *Chemical model.* Thomas[15] has suggested that the formation of carbon during the combustion of aliphatic hydrocarbons occurs through the free radical polymerization of C_1 and C_2 species, such as CH_3, CH_4, C_2H_2 etc., to form, first, conjugated polyene radicals, followed by cyclization to polybenzenoid radicals. The C:H ratio of the resulting polynuclear aromatic hydrocarbons should increase with crystallite size, as pointed out by Digonskii and Krylov[16] and confirmed by Cullis et al for carbon obtained by the pyrolysis of acetylene over silica[17]. The efficiency of Pt and Ni substrates as dehydrogenation catalysts may, therefore, be an important factor in the formation of highly graphitic carbon by pyrolysis of hydrocarbons. The high reaction velocities attainable during free radical polymerization make this model very attractive when considering the formation of flame carbon, which occurs typically within milliseconds. The production of crystalline graphite, however, requires highly mobile (i.e. low molecular weight) species with a long lifetime.

4.6.2 *Thin film model.* If the final product of the dehydrogenation of acetylene were a single carbon atom (or pair of atoms) and if such atomic carbon were mobile, then nucleation (either homogeneous or at preferred sites) followed by growth could occur, as in the formation of thin metal films by vacuum deposition. One would expect atomic carbon of this type to be extremely active chemically, resulting in a low surface mobility. That this is not necessarily so is shown by the experiments of Irving and Walker[7], in which carbon was vacuum evaporated on to foils of a number of metals (including Pt) held at 1000°C. The resulting films, especially on Pt, were considerably more graphitic than those deposited at room temperature, even though the deposition rate (between 1 and 10 A/sec) was somewhat higher than that used here (between 0·5 and 2·5 A/sec.).

4.6.3 *Metallurgical model.* Since carbon is being produced at the metal surface, the concentration gradient set up will cause it to diffuse normally to the surface. Nickel dissolves 0·23 wt.% (1·1 at. %) of carbon at 1000°C[18]. Solubility values are not available for the Pt–C system at this temperature, but Collier *et al.*[19] estimate about 0·25 wt.% (4 at. %) at the (reduced) melting point of 1734°C. Thus significant amounts of carbon are taken into solution in Ni and Pt and are known to be precipitated as graphite on cooling.

It should be born in mind, however, that the thermal inertia of a thin metal foil is very small; and cooling from 1000°C to room temperature would take a few seconds at most. Even if back diffusion of the carbon to the surface could take place as quickly as this, the conditions would hardly be ideal for the formation of well-ordered crystalline graphite, which requires slow precipitation of carbon from solution. Back diffusion to the surface would, of course, take place most rapidly along grain boundaries, which could account for their decoration at the surface. A serious difficulty arises, however, in those cases where grain boundary migration has taken place; and both positions of the grain boundary are decorated. In view of what has been said earlier, it is difficult to say with certainty which site corresponds to the final position of the boundary, but it is obvious that only one can do so. Yet a back diffusion mechanism could only operate at the very end of pyrolysis, during the cooling period, leading to decoration at only one position of the boundary, viz the final one.

5. CONCLUSIONS

Single crystal graphite is formed when acetylene is pyrolyzed over Pt and Ni at 1000°C.

Prior thermal annealing of the substrate influences the nucleation and growth of the deposit through kink site and step formation.

It is not yet clear whether there is an epitaxial relation between overgrowth and substrate.

A solution and reprecipitation model for the formation of graphite in this system is untenable. Two possible mechanisms remain—surface diffusion of atomic carbon species or polymerization and aromatization of short chain hydrocarbons.

Acknowledgements—We should like to thank the U.S. Atomic Energy Commission for their support on Contract No. AT(30–1)–1710 and also acknowledge the considerable help we have received from Dr. D. Gibbon and the Mineral Constitution Laboratory, Pennsylvania State University.

REFERENCES

1. Austerman S. B., Myron S. M. and Wagner J. W., *Carbon* **5**, 549 (1967).
2. Acheson R. G., U.S. Pat. Nos. 568328, 617979, 645285, 711031.
3. Diefendorf R. J., *J. Chim. Phys.* **57**, 815 (1960).
4. Presland A. E. B. and Hedley J. A., *J. Nucl. Mater.* **10**, 99 (1963).
5. Thomas J. M. and Walker P. L. Jr., *J. Chem. Phys.* **41**, 587 (1964).
6. Banerjee B. C., Hirt T. J. and Walker P. L. Jr., *Nature* **192**, 450 (1961).
7. Irving S. M. and Walker P. L. Jr., *Carbon* **5**, 399 (1967).
8. Karu A. E. and Beer M., *J. Appl. Phys.* **37**, 2179 (1966).
9. Porter G., *Combustion Researches and Reviews*, p. 108. Agard (1955).
10. Allpress J. G. and Sanders J. V., *Phil. Mag.* **9**, 645 (1964).
11. Barrett C. S., *Structure of Metals*, p. 457. McGraw-Hill, New York (1952).
12. Nelson J. P. and Riley D. P., *Proc. Phys. Soc.* **57**, 477 (1945).
13. *Handbook of Thermophysical Properties of Solid Materials*, Vol. 1, p. 461. Pergamon Press, Oxford (1961).
14. Freise E. J. and Kelly A., *Phil. Mag.* **8**, 1519 (1963).
15. Thomas A., *Combust. Flame* **6**, 46 (1962).
16. Digonskii V. V. and Krylov V. N., *J. Appl. Chem., USSR* **33**, 725 (1960).
17. Cullis C. F., Presland A. E. B., Read I. A. and Trimm D. L., *2nd Conf. on Industrial Carbon and Graphite*, p. 195. Society of Chemical Industry, London (1965).
18. Hansen M., *Constitution of Binary Alloys*, p. 374. McGraw-Hill, New York (1958).
19. Hansen M., *Constitution of Binary Alloys*, p. 377. McGraw-Hill, New York (1958).